*Human Molecular Genetics*, 2018, Vol. 27, No. 8 1343–1352

**doi: 10.1093/hmg/ddy045**
Advance Access Publication Date: 8 February 2018
Original Article

ORIGINAL ARTICLE

# Sema3a plays a role in the pathogenesis of CHARGE syndrome

Roser Ufartes[1,†], Janina Schwenty-Lara[2,†], Luisa Freese[1], Christiane Neuhofer[1], Janika Möller[2], Peter Wehner[3], Conny M.A. van Ravenswaaij-Arts[4], Monica T.Y. Wong[4], Ina Schanze[5], Andreas Tzschach[6], Oliver Bartsch[7], Annette Borchers[2,*,#] and Silke Pauli[1,*,#]

[1]Institute of Human Genetics, University Medical Center Göttingen, 37073 Göttingen, Germany, [2]Department of Biology, Molecular Embryology, Philipps-Universität Marburg, 35043 Marburg, Germany, [3]Department of Developmental Biochemistry, Georg August University Göttingen, 37077 Göttingen, Germany, [4]Department of Genetics, University of Groningen, University Medical Center Groningen, 9700 RB Groningen, The Netherlands, [5]Institute of Human Genetics, University Medical Center Magdeburg, 39120 Magdeburg, Germany, [6]TU Dresden, Faculty of Medicine Carl Gustav Carus, Institute for Clinical Genetics, 01307 Dresden, Germany and [7]Institute of Human Genetics, Johannes Gutenberg University Mainz, University Medical Centre, 55131 Mainz, Germany

*To whom correspondence should be addressed at: Department of Biology, Molecular Embryology, Philipps-Universität Marburg, Karl-von-Frisch-Str. 8, 35043 Marburg, Germany. Tel: +49 6421 2821503; Fax: +49 6421 2821538; Email: borchers@uni-marburg.de (A.B.); Institute of Human Genetics, University Medical Center Göttingen, Heinrich-Düker-Weg 12, 37073, Göttingen, Germany. Tel: +49 551 397589; Fax: +49 551 399303; Email: spauli@gwdg.de (S.P.)



## Abstract

CHARGE syndrome is an autosomal dominant malformation disorder caused by heterozygous loss of function mutations in the chromatin remodeler *CHD7*. Chd7 regulates the expression of *Sema3a*, which also contributes to the pathogenesis of Kallmann syndrome, a heterogeneous condition with the typical features hypogonadotropic hypogonadism and an impaired sense of smell. Both features are common in CHARGE syndrome suggesting that *SEMA3A* may provide a genetic link between these syndromes. Indeed, we find evidence that *SEMA3A* plays a role in the pathogenesis of CHARGE syndrome. First, Chd7 is enriched at the *Sema3a* promotor in neural crest cells and loss of function of Chd7 inhibits *Sema3a* expression. Second, using a *Xenopus* CHARGE model, we show that human *SEMA3A* rescues Chd7 loss of function. Third, to elucidate if *SEMA3A* mutations in addition to *CHD7* mutations also contribute to the severity of the CHARGE phenotype, we screened 31 *CHD7*-positive patients and identified one patient with a heterozygous non-synonymous *SEMA3A* variant, c.2002A>G (p.I668V). By analyzing protein expression and processing, we did not observe any differences of the p.I668V variant compared with wild-type SEMA3A, while a pathogenic SEMA3A variant p.R66W recently described in a patient with Kallmann syndrome did affect protein secretion. Furthermore, the p.I668V variant, but not the pathogenic p.R66W variant, rescues Chd7 loss of function in *Xenopus*, indicating that the p.I668V variant is likely benign. Thus, SEMA3A is part of an epigenetic loop that plays a role in the pathogenesis of CHARGE syndrome, however, it seems not to act as a common direct modifier.

[†]These authors contributed equally to this work.
[#]These authors are co-last authors.
**Received:** December 20, 2017. **Revised:** February 2, 2018. **Accepted:** February 2, 2018

## Introduction

Semaphorins are transmembrane or secreted proteins, which were originally identified as guidance factors controlling axonal pathfinding during the development of the nervous system (1). The large family of semaphorins was classified into eight groups according to structural similarities (2). Semaphorin-3A (MIM 603961) belongs to Subgroup 3, a group of secreted proteins playing a role in neural crest cell and axon guidance. A function of Sema3a as guidance factor controlling morphogenetic processes, like the migration of neural crest cells, is well established (3–6). Recently, it was demonstrated that *SEMA3A* mutations contribute to the phenotype of Kallmann syndrome (HH16; MIM 614897), a genetically heterogeneous congenital disorder, characterized by a combination of hypogonadotropic hypogonadism and impaired sense of smell (7–9). These two features are owing to migration defects of GnRH producing cells and olfactory neurons on their way from the olfactory placode to the hypothalamus and bulbus olfactorius (10,11). Therefore, it is not surprising that many of the genes linked to Kallmann syndrome have a function in axon growth and guidance. Indeed, several *SEMA3A* mutations have been detected in patients with Kallmann syndrome (8,9). A disease modifying effect of the *SEMA3A* mutations or a digenic/oligenic inheritance was postulated because *SEMA3A* mutations alone seem not to be sufficient to produce the Kallmann syndrome phenotype (9).

Hypogonadotropic hypogonadism and an impaired sense of smell are two features, which are also frequently observed in CHARGE syndrome (12–15), a congenital malformation disorder affecting several organ systems. CHARGE syndrome is caused by heterozygous loss of function mutations in *CHD7* (MIM 608892), a chromodomain helicase DNA-binding protein required for ATP-dependent chromatin remodeling. Besides causing CHARGE syndrome, heterozygous *CHD7* mutations (HH5; MIM 612370) have also been identified in a minority of Kallmann syndrome patients, which exhibit features reminiscent of a mild CHARGE phenotype, like for example hearing loss. Therefore, it has been suggested that Kallmann syndrome, caused by *CHD7* mutations, and CHARGE syndrome are allelic disorders, whereby Kallmann syndrome represents the mild end of the phenotypic spectrum (16). Consistent with this hypothesis, we could recently demonstrate a regulatory loop between Chd7 and Sema3a using a Chd7-deficient mouse model ($Chd7^{Whi/Whi}$) and by performing knockdown experiments in *Xenopus laevis*. In both model systems a downregulation of Chd7 led to a reduction in the Sema3a expression (17). Further support for an epigenetic regulation of Class 3 semaphorins by Chd7 comes from a genome-wide transcriptional analysis of mice with a conditional ablation of Chd7 in early cardiogenic mesoderm (18). Interestingly, bi-allelic loss of function mutations in *SEMA3A* were recently discovered to cause a syndrome with short stature, skeletal anomalies, congenital heart defects, a micropenis, and variable additional anomalies (19,20). Although this syndrome differs from CHARGE syndrome, an overlap of the affected tissues could be observed. Taken together these data support a role of SEMA3A in the pathogenesis of CHARGE syndrome. However, so far pathogenic *SEMA3A* variants have not been identified as the causes of CHARGE syndrome in patients lacking a pathogenic *CHD7* mutation. Therefore, the aim of this study was to investigate a possible epigenetic link between CHD7 and SEMA3A and the role of SEMA3A in the pathogenesis of CHARGE syndrome in a wider sense.

## Results

### *In vivo* evidence for an epigenetic control of Sema3a expression by Chd7

To analyze the role of SEMA3A in the pathogenesis of CHARGE syndrome, we used the *Xenopus in vivo* model system. Previously, it was shown that loss of function of Chd7 in *Xenopus* recapitulates all major features of CHARGE syndrome (21). Embryos injected with Morpholino oligonucleotides (MO) blocking Chd7 protein translation showed defects in the transcriptional circuitry required for neural crest specification and migration. At late tadpole stages Chd7 knockdown led to severe malformations of the craniofacial cartilage, coloboma of the eyes as well as heart defects (21). Similar—although less severe—defects were observed if embryos were injected with an MO blocking the translation of the Sema3a protein (Supplementary Material, Fig. S1), supporting previous data suggesting that Sema3a is one of the genes whose expression is regulated by Chd7 (17,18). Furthermore, to analyze if Sema3a can rescue the craniofacial malformations of Chd7 morphants, *Xenopus* embryos were injected in one blastomere at the two-cell stage resulting in embryos where the injected side can be directly compared with the uninjected control side (Fig. 1A). Embryos were injected either with chd7 MO or control MO in combination with *lacZ* RNA for lineage tracing. For rescue experiments wild-type (wt) human *SEMA3A* RNA was co-injected. Craniofacial malformations were phenotypically analyzed at tadpole stages (Fig. 1A). As expected, Chd7 morphants showed severe craniofacial defects on the injected side, while craniofacial structures developed normally on the control side (Fig. 1B and C). These defects could be partially rescued by concomitant overexpression of human *SEMA3A*. Thus, these data are consistent with a model whereby Chd7 activates Sema3a expression and support a role of SEMA3A as a modifying factor in CHARGE syndrome.

### *SEMA3A* variants are not common disease-modifying factors in CHARGE syndrome

CHARGE syndrome patients show a high variability in their clinical presentation, ranging from mild to severe, which may be caused by mutations in additional modifying factors. To elucidate if typically affected CHARGE patients carry, in addition to a pathogenic *CHD7* mutation, a *SEMA3A* variant acting as a modifier, we screened 31 *CHD7*-positive CHARGE patients grouped into typical or atypical according to the clinical criteria of Blake and/or Verloes (22,23). An overview of the clinical details is given in Supplementary Material, Table S1. The coding region of *SEMA3A* (NM_006080.2) was sequenced in all 31 patients. In one patient we identified the non-synonymous *SEMA3A* variant c.2002A>G (p.I668V) in a heterozygous state (Patient 9; Supplementary Material, Table S1). This mutation leads to an amino acid substitution from Isoleucin to Valine at position 668 and was recently also described in one out of 45 *CHD7*-negative CHARGE patients screened for *SEMA3A* variants (17). The variant is not listed in the Exome Aggregation Consortium (ExAC) database and its functional relevance is currently unknown. Therefore, we turned again to the *Xenopus* system to test if this variant is able to rescue the craniofacial defects observed in Chd7 morphant embryos (Fig. 1B and C). In addition, we tested the SEMA3A variant p.R66W, which was recently identified in a heterozygous state in patients with Kallmann syndrome and suggested to affect SEMA3A secretion. Co-expression of the

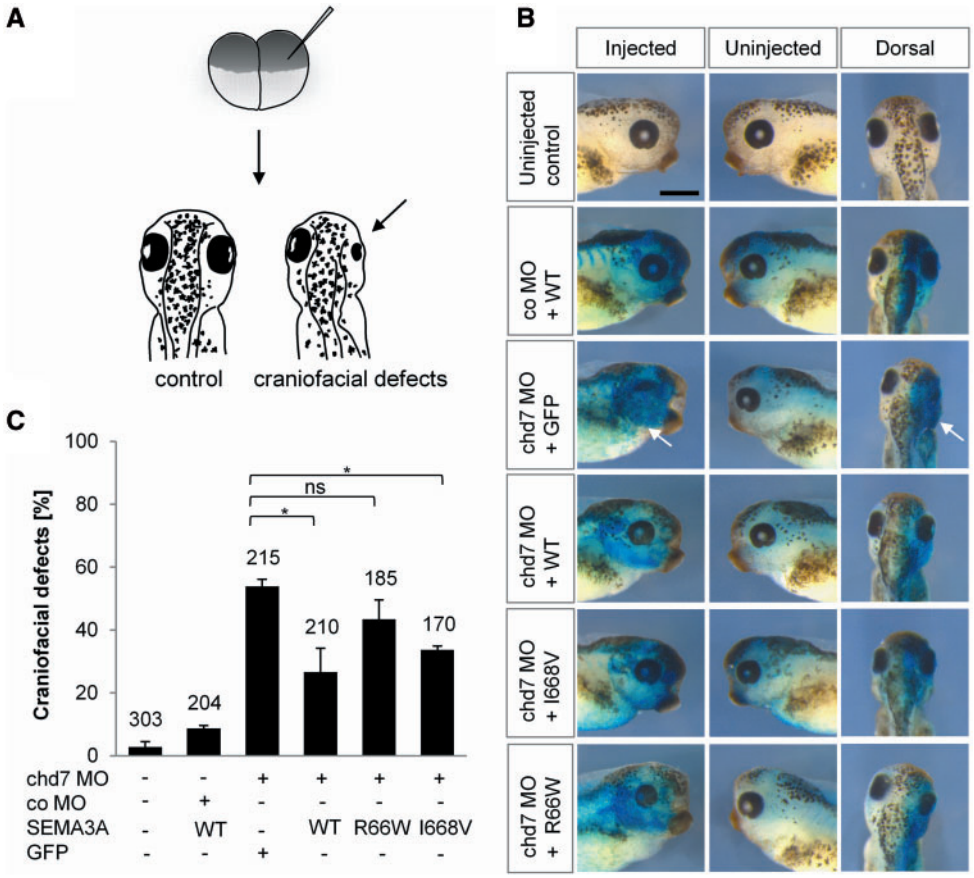


**Figure 1.** Wild-type and p.I668V mutant Sema3a partially rescue craniofacial defects caused by Chd7 loss of function. (**A**) Embryos were injected with 5 ng of the respective MO in combination with 250 pg *SEMA3A* RNA or *GFP* RNA as a control into one blastomere at the two-cell stage. A 75-pg *lacZ* RNA was co-injected for lineage tracing. Cartilage morphology was analyzed at tadpole stages (Nieuwkoop and Faber stages 38–40). Arrow indicates craniofacial defects on the injected side. (**B**) CHD7 knockdown causes severe craniofacial defects (white arrows). Co-injection of *SEMA3A* with the chd7 MO can partially rescue the craniofacial defects caused by Chd7 loss of function. A similar effect is seen using the p.I668V SEMA3A variant. In contrast, the p.R66W SEMA3A variant does not show a significant rescue effect. LacZ staining (blue) marks injected sides (left panels). Middle panels show the uninjected side, right panels present a dorsal view of the head region of the respective embryos. (**C**) Graph summarizing the mean ± s.e.m. percentage of craniofacial defects of three independent experiments. The number of injected embryos is indicated for each experimental condition. *$P < 0.05$ (Student's *t*-test) and ns, no significant difference.

human SEMA3A variant p.I668V significantly improved the *Xenopus* Chd7 loss of function phenotype, indicating that this mutant is not pathogenic. In contrast, co-expression of the p.R66W variant did not rescue the craniofacial defects caused by Chd7 knockdown, supporting the notion that this mutation has a pathogenic effect (Fig. 1B and C).

Next, we analyzed if the SEMA3A mutations affect protein expression or secretion and if this may contribute to their pathogenic or benign effects. Recently, the p.R66W variant was suggested to cause defects in protein secretion. Hanchate et al. showed that conditioned medium from transfected COS-7 cells contains secreted wt SEMA3A protein, but not the p.R66W variant (8). However, as the intracellular SEMA3A expression was not analyzed, it remains unclear if this result was caused by an expression or secretion defect. Therefore, here we used cell lysates as well as media of transfected HEK293 cells to analyze the processing and secretion of different SEMA3A protein variants. For Class 3 semaphorins monomeric, dimeric, and processed forms have been described (24). Figure 2A and B shows schematic representations of full-length Sema3a, the predicted processing sites, and the potential isoforms, which may result from proteolytic cleavage as well as dimerization. In order to check for monomeric and dimeric SEMA3A isoforms, concentrated media and cell lysates were analyzed in presence or absence of the reducing agent DTT. In presence of DTT monomeric isoforms of ~85/87 kDa (monomer p85 or p87) and ~61 kDa (monomer p61) were detected in the concentrated media; without DTT dimeric isoforms of ~170/174 kDa (dimer p85:p85 or p87:87) and a weak band of ~122 kDa, corresponding to the dimeric form p61:61, were detected as well as monomers of ~82 kDa (p82) and ~61 kDa. In lysates without DTT a weak band corresponding to the dimeric isoform of ~170/174 kDa, as well as the dimeric isoform of ~122 kDa (p61:p61) were detected. In cell lysates with DTT only the monomeric isoform of ~85/87 kDa was observed (Fig. 2B). We did not detect any alterations in expression or processing pattern for wt SEMA3A or the SEMA3A variants p.R66W and p.I668V (Fig. 2C). SEMA3A is a glycosylated protein. To determine if the mutations have an influence on the glycosylation status of SEMA3A, we treated the cells with tunicamycin, an inhibitor of N-linked glycosylation. In presence of tunicamycin the variant p.R66W showed two bands, likely corresponding to the glycosylated and unglycosylated forms, while for wt SEMA3A and the p.I668V variant only a single band, corresponding to the unglycosylated form, could be detected. In addition, Western blot analysis of concentrated media from transfected HEK293 cells, producing HA-tagged wt

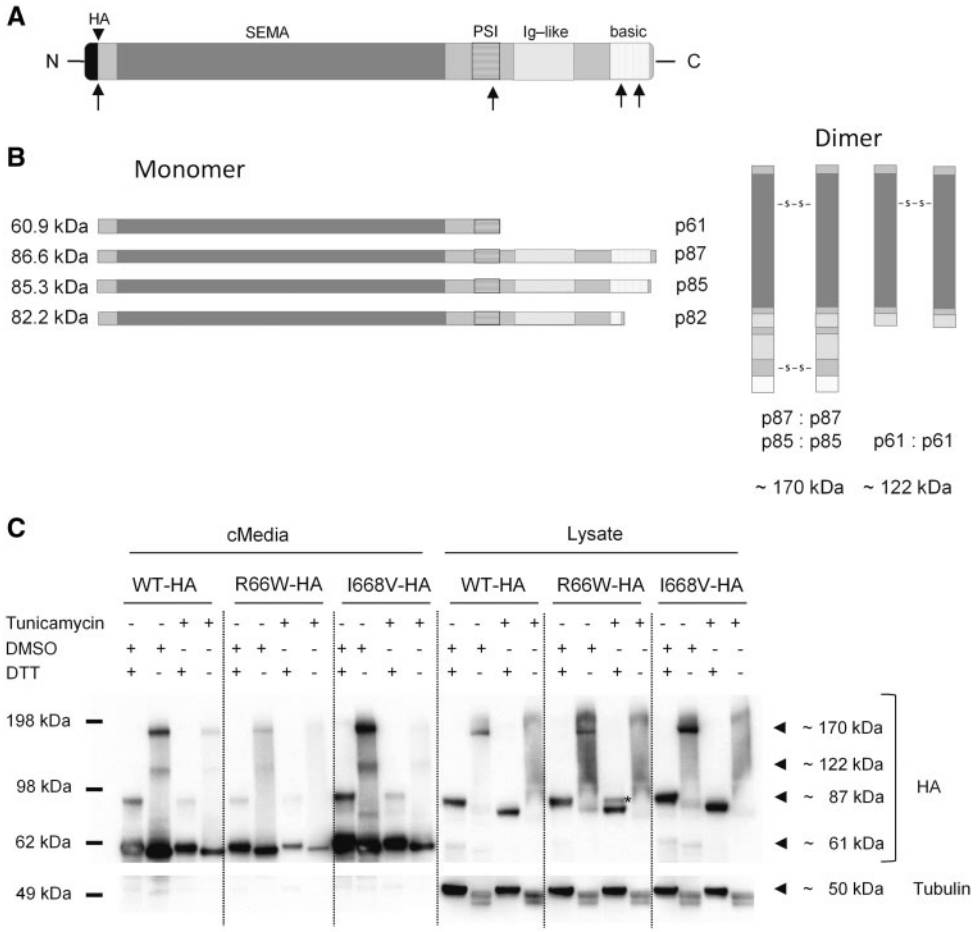


**Figure 2.** The SEMA3A variant p.I668V shows no expression, processing, and secretion defect in HEK293 cells. (**A**) Schematic representation of the SEMA3A protein: the position of the signal peptide (black), the SEMA domain (dark grey), the Plexin-Semaphorin-Integrin domain (PSI, horizontally striped), the immunoglobulin-like domain (diagonally striped), the basic domain (dotted), and the predicted processing sites 1, 2 and 3 (black arrowheads) are indicated. A triangle marks the position of the included HA-tag. (**B**) Schematic representation of the different SEMA3A isoforms generated by proteolytic processing and dimerization. Predicted molecular weights of the cleavage products are shown in kDa. (**C**) Overexpression and Western blot analysis of wild-type (wt) SEMA3A and the p.R66W and p.I668V variants in HEK293 cells. Protein expression or processing was not affected in the presence or the absence of the reducing agent DTT. In the presence of the glycosylation inhibitor tunicamycin, the variant p.R66W showed two bands, likely corresponding to the glycosylated (indicated by a star) and unglycosylated SEMA3A forms. For wt SEMA3A and the p.I668V variant only a single band, corresponding to the unglycosylated form, could be detected. The detection of α-tubulin (~50 kDa) served as loading control for the cytoplasmic fraction.

SEMA3A or HA-tagged mutant SEMA3A, indicates a secretion defect of variant p.R66W in comparison to the wt or p.I668V mutant (Fig. 2C). Thus, these biochemical data support the pathogenic effect of the p.R66W variant, while the p.I668V variant is likely benign.

## Sema3a is expressed, processed, and secreted by the cranial neural crest cell line O9–1

Although Class 3 semaphorins are known guidance factors that attract or repel neural crest cells, recent data indicate that they are also expressed in neural crest cells. For example, Sema3c expression was demonstrated in a subpopulation of cardiac neural crest cells by *in situ* hybridization of *Wnt1-Cre-Rosa*$^{Yfp}$ outflow tracts, suggesting that cardiac neural crest cells provide an essential source for Sema3c (25). To elucidate if Sema3a is also expressed in neural crest cells, we performed an RT-PCR analysis for Sema3a, Sema3c, and their receptors PlexinA1 (PlxnA1), Neuropilin-1 (Nrp1) and Neuropilin-2 (Nrp2) in the murine cranial neural crest cell line O9–1 established by Ishii *et al.* (26). We could show that O9–1 cells express Sema3a and Sema3c as well as their receptors (Supplementary Material, Fig. S2). These results were confirmed by Western blot analysis using a Sema3a-antibody, which revealed the same monomeric and dimeric endogenous Sema3a isoforms as already observed for overexpressed SEMA3A in HEK293 cell lysates and media (Fig. 3B; see also Fig. 2C). Furthermore, these data were confirmed by transfecting a HA-tagged Sema3a full-length construct and performing Western blot analysis using an anti-HA antibody. In summary, our results demonstrate that Sema3a is expressed, processed, and secreted by O9–1 cells, suggesting that neural crest cells provide a source of Sema3a.

## Chd7 binds to the *Sema3a* promoter and regulates Sema3a expression in murine and *Xenopus* neural crest cells

Recently, we showed by microarray analysis and quantitative reverse transcription PCR (qRT-PCR) on RNA from *Chd7*-deficient mouse embryos that a downregulation of *Chd7* leads to a

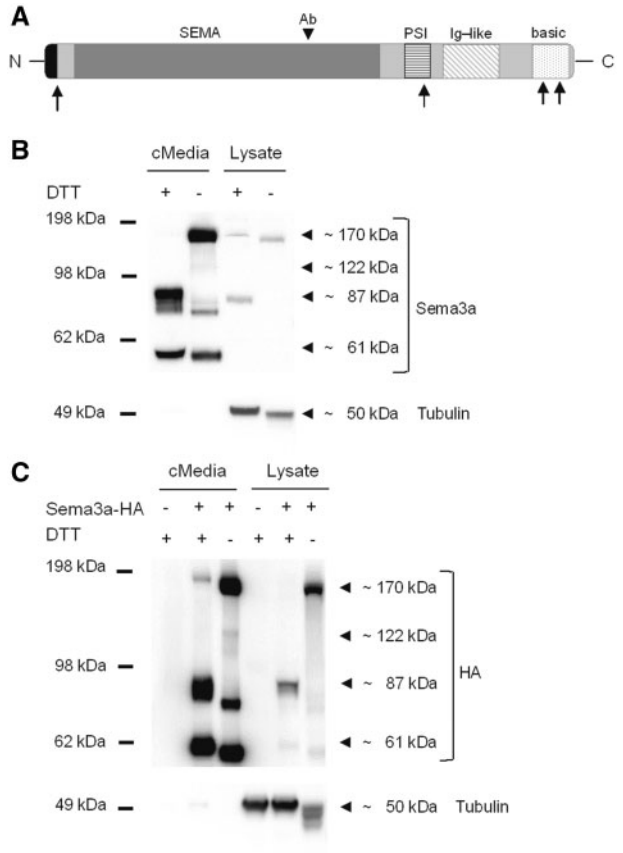


**Figure 3.** Sema3a is differentially processed and secreted in O9–1 cells. (**A**) Schematic representation of the Sema3a protein (see also Fig. 2) indicating the epitope targeted by the Sema3a antibody. (**B**) Western blot analysis using an anti-Sema3a antibody to analyze Sema3a expression of cell lysates and media of O9–1 cells. p87-Sema3a is detected in the cytoplasm as well as in the media, while the p87:p87-Sema3a dimers (~174 kDa) are only detected in absence of DTT. p61-Sema3a is exclusively detected in the media (with or without DTT treatment). As a cytosolic control an anti-α-tubulin antibody was used (~50 kDa). (**C**) Western blot analysis using an anti-HA-antibody to analyze the expression of a HA-tagged Sema3a plasmid in the cytosol and media of O9–1 cells, confirming the endogenous expression pattern.

downregulation of Sema3a (17). In order to determine whether this regulatory loop also plays a role in neural crest cells, we analyzed Sema3a expression in explanted *Xenopus* neural crest cells. Neural crest explants from *Xenopus* embryos, injected either with 10 ng control MO or chd7 MO, were dissected at premigratory stages and Sema3a expression was analyzed by RT-PCR (Fig. 4A). RT-PCR showed that *sema3a* expression can be detected in both control MO and chd7 MO injected neural crest cells. However, compared with control cells, *sema3a* expression was significantly reduced in chd7 knockdown neural crest cells. To further confirm these data in murine O9–1 cells, which also express Sema3a and Chd7, O9–1 cells were transfected with two different short interfering RNAs against *Chd7*. RNA was isolated from O9–1 cells 48 h after siRNA transfection and analyzed by qRT-PCR. Compared with O9–1 cells transfected with a control siRNA, a reduced relative *Chd7* expression between 65 and 70% was observed in O9–1 cells transfected with siRNA against *Chd7* (Fig. 4B). Thus, downregulation of *Chd7* expression leads to a significant reduction in the *Sema3a* expression in *Xenopus* neural crest cells as well as in the murine cranial neural crest cell line O9–1.

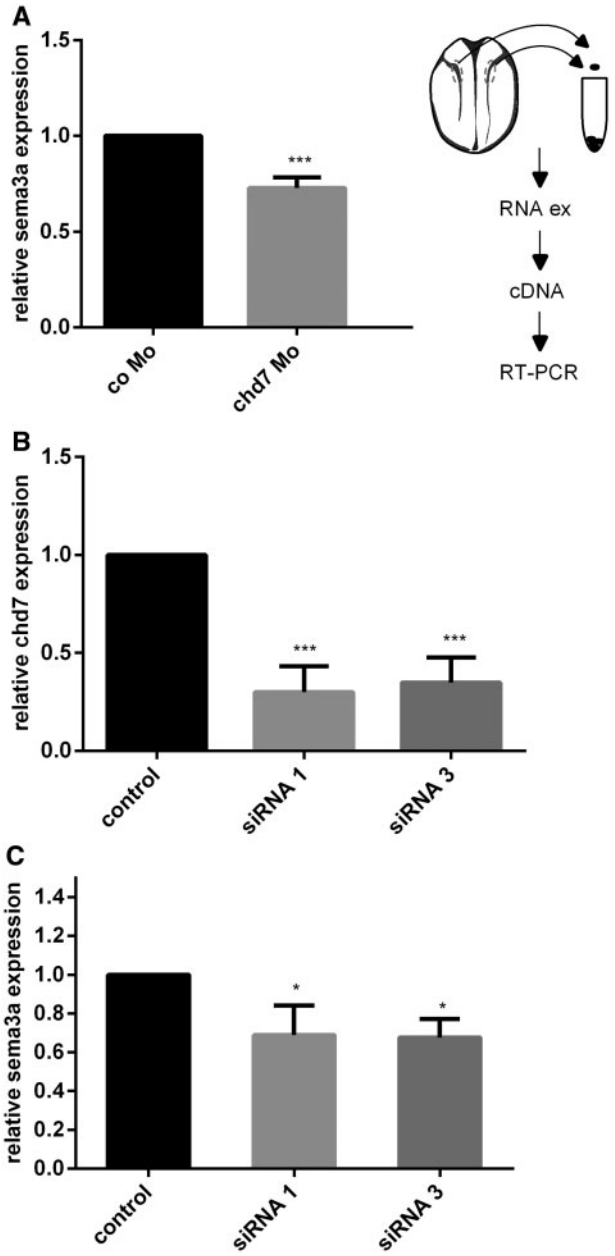


**Figure 4.** Sema3a is regulated by Chd7 in *Xenopus laevis* neural crest explants and the murine neural crest cell line O9–1. (**A**) CHD7 loss of function significantly reduces *sema3a* expression in *Xenopus* cranial neural crest cells. *Xenopus* embryos were injected with 10 ng control MO or chd7 MO, and cranial neural crest cells were dissected and analyzed by RT-PCR at premigratory stages as indicated in the schematic overview (right). The graph represents the relative *sema3a* expression normalized to *histone H4* expression. (**B**) Chd7 knockdown by siRNA in O9–1 cells. *Chd7* expression was significantly reduced in O9–1 cells transfected with two different short interfering RNAs against *Chd7* (siRNA1 and siRNA2). (**C**) *Chd7* knockdown leads to a reduced *Sema3a* expression in O9–1 cells.

Finally, we used chromatin immunoprecipitation (ChIP) for Chd7 to determine if Chd7 interacts with the promoter region of *Sema3a*. Therefore, ChIP followed by qRT-PCR on chromatin from O9–1 cells was performed. As a positive control we used *Sema3c* and *Nkx2.5-Ar2*, while an IgG antibody or no antibody was used as negative controls for the immunoprecipitation. These experiments confirmed an enrichment of Chd7 at the promoter region of *Sema3a*, *Sema3c*, and *Nkx2.5-Ar2* (Fig. 5).

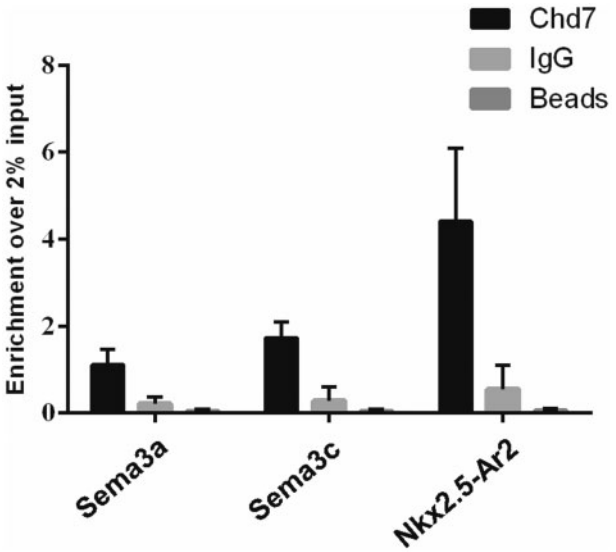


**Figure 5.** Direct regulation of Sema3a by Chd7 in O9–1 neural crest cells. CHIP assays were performed using an anti-Chd7 antibody or IgG or no antibody as negative controls. Using the anti-Chd7 antibody, Chd7 binding to the Sema3a promotor region was shown. Sema3c and Nkx2.5-Ar2 served as positive controls.

Thus, these data support an epigenetic link, by which Chd7 activates the expression of Sema3a, and indicates a role of SEMA3A in the pathogenesis of CHARGE syndrome.

## Discussion

Neural crest cells are multipotent migratory cells that migrate from the dorsal region of the neural tube to several regions of the developing embryo. Neural crest cells give rise to diverse cell types, such as peripheral neurons, glia, craniofacial chondrocytes, smooth muscle, and pigment cells (27). Furthermore, neural crest cells contribute to parts of the cardiac outflow tract. Syndromes, which are caused by defects in neural crest development, are commonly referred to as so called 'neurocristopathies'. Some of the defining features of CHARGE syndrome, like craniofacial defects, inner ear malformations, cleft palate and conotruncal heart defects, suggest that it belongs to the neurocristopathies. Consistently, it was shown that *CHD7*, the gene mutated in CHARGE syndrome patients, is required at specific stages of neural crest development. For example, an essential role of Chd7 was shown in the activation of a transcriptional network, including Sox9, Twist, and Snail2, which is necessary for neural crest migration and specification (21). Moreover, Chd7 seems to be involved in later steps of neural crest migration and differentiation. By performing a genome-wide microarray expression analysis on wt and Chd7-deficient mouse embryos, we could recently demonstrate that a reduction of *Chd7* expression leads to differences in the expression levels of genes involved in neural crest cell migration, guidance, and ectoderm to neural crest cell interactions (17). One of these genes is *Sema3a*, a Class 3 semaphorin known to be involved in the pathogenesis of Kallmann syndrome and mutated in an autosomal recessive type of syndromic short stature.

To elucidate the functional role of SEMA3A in the pathogenesis of CHARGE syndrome, we used *Xenopus laevis* as a model organism. We showed that loss of Sema3a phenocopies aspects of the Chd7 loss of function phenotype in *Xenopus* neural crest development. Interestingly, these effects are less severe compared with Chd7 loss of function, which may be explained by the fact that sema3a comprises only one of the genes affected by Chd7 loss of function. Furthermore, by performing Chd7 knockdown experiments in *Xenopus laevis* embryos, we were able to partially rescue the CHARGE phenotype by injection of human *SEMA3A* wt RNA, confirming the hypothesis of a functional relevance of SEMA3A in the pathomechanism of CHARGE syndrome.

For CHARGE syndrome a high inter- and intra-familial variability of the clinical presentation was observed, suggesting that mutations in additional genes can act as modifiers by enhancing or suppressing the CHD7 phenotype. Thus, we asked if *SEMA3A* variants are a modifying factor in CHARGE syndrome. To this end we screened for *SEMA3A* variants in 31 CHARGE patients with a pathogenic *CHD7* mutation, grouped into having a typical or atypical phenotype according to the clinical criteria from Blake and/or Verloes (22,23). In one patient we identified the non-synonymous variant c.2002A>G (p.I668V) in *SEMA3A* in a heterozygous state. The functional relevance of this variant is unknown. Therefore, we performed further analysis to elucidate the character of this variation and the c.196C>T (p.R66W) variant, found in a patient with Kallmann syndrome and recently described as pathogenic owing to impaired secretion of the mutated protein (8). Using transfected HEK293 cells no expression, processing, glycosylation or secretion defects could be observed for the p.I668V variant compared with overexpressed wt SEMA3A, suggesting that this variant is not pathogenic. In contrast, for the p.R66W we observed a secretion defect and abnormalities in the glycosylation pattern, which may indicate that the protein is misfolded and subsequently abnormally glycosylated. For example, N-glycans can serve as a tag for the endoplasmic reticulum (ER) chaperons to control the folding status of a protein. Correctly folded proteins can leave the ER, while misfolded proteins are subject to proteasome-mediated degradation (28). Therefore, it is possible that the secretion defect of the variant p.R66W is simply caused by an increase in degradation compared with wt SEMA3A. Confirming a pathogenic effect of the p.R66W variant, we find that the *Xenopus laevis* Chd7 loss of function phenotype cannot be rescued by overexpression of the SEMA3A variant p.R66W. In contrast, the variant p.I668V leads to a partial rescue, indicating that the p.I668V variant is benign. Thus, although SEMA3A variants play a role in the pathogenesis of Kallmann syndrome, our results suggest that SEMA3A variants are not common disease modifying factors in CHARGE syndrome. One explanation could be that a reduced CHD7 expression, like in CHARGE syndrome patients, leads to a downregulation of SEMA3A. Therefore, an additional mutation in *SEMA3A* may not add to the pathogenic effect. Interestingly, autosomal recessive loss of function mutations in *SEMA3A* were recently described to be causative for a syndromic form of short stature in two unrelated affected boys with postnatal short stature, skeletal abnormalities, hypogonadotropic hypogonadism, micropenis, muscular hypotonia, delayed motor development, cardiovascular anomalies, and mild facial dysmorphism (19,20). Although the disorders are distinct, several clinical features of the SEMA3A syndromic short stature phenotype overlap with CHARGE syndrome. For example skeletal abnormalities like scoliosis, kyphosis or abnormalities of the vertebral bodies and costal defects, limb anomalies as well as short stature and hypogonadotropic hypogonadism with micropenis were described in CHARGE syndrome patients (29–31).

Sema3a belongs to a subgroup of secreted proteins of the semaphorin family, which bind to plexin or neuropilin receptors

in order to mediate repulsive or attractive signals to guide neural crest cells to their destination. For Sema3c, another Subgroup 3 semaphorin, it was recently shown that a subpopulation of cardiac neural crest cells does not respond to guidance factors as expected. Instead, it was demonstrated that these cardiac neural crest cells express Sema3c thereby offering a substantial source of Sema3c (25). To test if this is also the case for Sema3a, we performed expression analysis for Sema3a in the murine cranial neural crest cell line O9–1. Indeed, we could demonstrate that O9–1 cells express, process, and secrete Sema3a. Furthermore, the described regulatory loop between Chd7 and Sema3a could also be observed in O9–1 cells. A Chd7 knockdown by siRNA leads to a reduction of the Sema3a expression. This could also be confirmed in Chd7 morphant *Xenopus laevis* neural crest explants.

For Sema3c a direct transcriptional regulation through Chd7 was postulated because Chd7 was shown to localize at the *Sema3c* promoter (18). To investigate if this is also the case for Sema3a, we performed a ChIP for Chd7, followed by qRT-PCR on chromatin from O9–1 cells, and could observe an enrichment of Chd7 at the promoter region of *Sema3a*, identifying *Sema3a* as a direct target of Chd7.

Although it seems that *SEMA3A* variants are not common modifying factors in CHARGE syndrome, our results suggest that Sema3a is part of a regulatory network that is compromised in CHARGE syndrome. As Sema3a expression is regulated by Chd7, pathogenic mutations in CHD7 also affect SEMA3A expression and function. Thereby, SEMA3A likely plays an important role in the pathogenesis of CHARGE syndrome by acting as a downstream CHD7 target.

## Materials and Methods

### Cell culture, treatment and transient transfection

HEK293 cells were cultured in Dulbecco's modified Eagle's medium (DMEM) [PAN-Biotech, supplemented with 10% fetal bovine serum (FBS) (PAN-Biotech)], 1× MEM Non-Essential Amino Acids (NEAA) (Gibco) and 1% penicillin/streptomycin (Gibco). O9–1 mouse cranial neural crest cells (Merck Millipore, Darmstadt) were grown in complete ES Cell Medium with 15% FBS and leukemia inhibitory factor (Merck Millipore) and 25 ng/ml fibroblast growth factor 2, human (FGF-2) (PeproTech). For transfection, $5.4 \times 10^6$ HEK293 cells were plated into T75 culture flasks (Greiner Bio-One) and $1 \times 10^6$ O9–1 cells were plated into culture plates (Ø 10 cm) (Nuclon A/S), which were precoated with 1:50 diluted Matrigel solution (Corning). After 24 h, when the cells reached ∼70–80% confluence, they were transfected with plasmid DNA using Opti-MEM I Reduced Serum Medium (Gibco) and Lipofectamine 2000 Transfection Reagent (Invitrogen) according to the manufacturer's instructions. After transfection, cells were grown for an additional 24 h in DMEM for HEK293 cells and in complete ES Cell Medium for O9–1 cells. For concentrating the media, the Vivaspin Turbo 15 columns (30 kDa MWCO, Sartorius) were used, after HEK293 cells and O9–1 cells were grown in DMEM with 1× NEAA and O9–1 cells with an additional 25 ng/ml FGF-2 for 24 h. For tunicamycin treatment, cells were treated for 16 h with 5 μg/ml tunicamycin (T7765, Sigma-Aldrich) or 0.05% dimethyl sulfoxide (DMSO) (Carl Roth). Before treatment, the transfection media was exchanged for tunicamycin or DMSO medium, respectively. Sixteen hours later, cells were harvested for further analysis. All experiments were performed three times.

### SEMA3A constructs and site-directed mutagenesis

The entire open reading frame of human wt *SEMA3A* as well as murine wt *Sema3a* was amplified by PCR and cloned into the pCMV-HA vector using the In-Fusion® HD Cloning Kit (Clontech) according to the manufacturer's protocol. For the *Xenopus laevis* experiments *SEMA3A* was cloned from the pCMV-HA vector into the pcDNA3.1/*myc*-His B vector using the In-Fusion® HD Cloning Kit (Clontech). To introduce the point mutations c.196C>T (p.R66W) and c.2002A>G (p.I668V), a site directed mutagenesis PCR, using QuikChange II XL Site-Directed Mutagenesis Kit (Agilent Technologies), was performed according to the manufacturer's protocol. Primer sequences can be sent on request.

Because semaphorin-3A is synthesized as an inactive precursor and undergoes proteolytic cleavage, we introduced a HA-tag (YPYDVPDYA) after the signal peptide of Sema3a (G25-K26) (24) by PCR site-directed mutagenesis. Plasmids were sequenced to validate the correct sequence. Primer sequences can be sent on request.

### Western blot analysis

To concentrate the media of O9–1 and HEK293 cells, Vivaspin Turbo 15 columns (30 kDa MWCO, Sartorius) were used. Thirty micrograms of protein or 18 μl concentrated medium were separated by a 4–12% NuPAGE Bis–Tris Gel (Invitrogen) and transferred to a nitrocellulose membrane (0.45 μm) (GE Healthcare) using a Tank system at 250 mA for 60 min at 4°C. Membranes were blocked with 5% milk/TBST (Carl Roth) for 60 min and afterwards incubated with appropriate primary antibodies overnight at 4°C. Rat anti-HA (11867431001, Sigma Aldrich) was used at a dilution of 1:1000 in 2% milk/TBST. Rabbit anti-Sema3a (ab23393, Abcam) was diluted 1:1000 in 2% milk/TBST. After washing, the membrane was incubated with the following secondary antibodies: anti-rat IgG peroxidase secondary antibody (31470, Pierce) at a dilution of 1:10 000 in 2% milk/TBST, goat IgG anti-rabbit (H + L)-HPRO (A8275, Sigma) at a dilution of 1:10 000 in 2% milk/TBST. The membrane was washed three times with TBST, Immobilon Western Chemiluminescent HRP Substrate (Merck Millipore) was applied to the membrane, and positive bands were detected using FluorChem® Q (Alpha Innotech). Protein quality was controlled using mouse anti-α-tubulin (T5168, Sigma Aldrich) at a dilution of 1:10 000 in 2% milk/TBST. The experiments were performed three times.

### Chromatin immunoprecipitation (ChIP)

ChIP analysis of O9–1 cells was performed at least three times as described before (32) with minor modifications. Cultured cells (around $6–8 \times 10^7$ cells) were crosslinked in two steps (33). First, cells were incubated with 5 mM DSG (sc-285455a, Santa Cruz) in PBS for 45 min. Next, the cells were washed twice with PBS and crosslinked with 1% formaldehyde (Carl-Roth) solution in PBS for 15 min and then stopped with 0.125 M glycine (Carl-Roth) for 5 min. Cells were washed twice with cold PBS and afterwards 2 ml cold PBS [proteinase inhibitor (Roche) and 1:1000 MG132 (474790, Calbioechem)] were added to the plate and cells were collected by scraping. After centrifugation at 1000×*g* at 4°C, the pellet was frozen or resuspended in 5 ml lysis Buffer [50 mM Tris–HCl pH 8.0, 3 mM $MgCl_2$, protease inhibitor complete 1:1000, MG132 and 1 mM PMSF (Sigma-Aldrich)]. Subsequently, the cells were lysed with 5 ml lysis Buffer with 1% NP-40. After

5 min on ice, cells were centrifuged at 1100×*g* at 4°C and the pellet was resuspended and incubated with NUC buffer (50 mM Tris–HCl pH 8.0, 5 mM $CaCl_2$) for 10 min on ice. A 100-µl 1% SDS was added and the cells were incubated for 5 min on ice. A 1.9-ml non-SDS buffer (10 mM Tris–HCl pH 8.0, 1 mM EDTA, 0, 5 mM EGTA and proteinase inhibitor) was added and the cell lysates were sonicated in 15 ml tubes using a Bioruptor sonicator (Diagenode) for 10 cycles at high power on ice (30 s on, 50 s off). This procedure was repeated six times and results in chromatin with an average DNA fragment size of 200–600 bp. After centrifugation at 10 000×*g*, the supernatant was collected, and the DNA concentration was measured using a NanoDrop 2000c (Peqlab). A 10 µg sheared chromatin was diluted in 500 µl Chip Buffer (0.1% SDS, 1.1% Triton X-100, 1.2 mM EDTA, 16.7 mM Tris–HCl, pH 8.0, 167 mM NaCl and proteinase inhibitor). A 10-µl sheared chromatin was frozen as an Input (2%), and 10 µg of anti-CHD7 antibody (ab31824, Abcam) or as a negative control either 10 µg of rabbit IgG (#2729, Cell Signaling) or non-antibody, was added. After overnight incubation at 4°C in rotation, 30 µl of ChIP-Grade Protein G Magnetic Beads (9006S, Cell Signaling) were added and the incubation was continued for 2 h. Protein G magnetic beads containing the immune complexes were washed twice with low salt buffer (0.1% SDS, 1% Triton X-100, 2 mM EDTA, 20 mM Tris–HCl pH 8, 0, 150 mM NaCl), twice with high salt buffer (0.1% SDS, 1% Triton X-100, 2 mM EDTA, 20 mM Tris–HCl pH 8.0, 500 mM NaCl), once with LiCl salt buffer (250 mM LiCl, 1% Igepal, 1% deoxycholic acid sodium salt, 1 mM EDTA, 10 mM Tris–HCl, pH 8.0) and once with TE buffer (10 mM Tris–HCl, pH 8.0, 1 mM EDTA). After the washing step, the immune complexes as well as 2% input were eluted and revers crosslinked with 200 µl Elution Buffer [1% SDS, 0.1 M $NaHCO^3$, 6 µl 5 M NaCl and 2 µl Proteinase K (10 mg/ml)] for 2 h at 62°C and 10 min at 95°C. DNA fragments were purified using spin columns (Invitek). The enrichment was analyzed by real-time PCR using locus-specific primers. Data were normalized to 2% input and compared with the enrichment at non-specific loci.

### Micromanipulation of *Xenopus laevis* embryos

*Xenopus laevis* embryos were obtained by *in vitro* fertilization and injected and cultivated as previously described (34). Stages were determined according to Nieuwkoop and Faber (35). Synthesis of capped sense RNA for injection was performed *in vitro* using the mMessage mMachine kit™ (Ambion, Thermo Fisher Scientific). Digoxigenin-labeled antisense RNA for *in situ* probes was generated with a DIG-RNA labeling kit (Roche). The following linearized plasmids were used for RNA synthesis: *lacZ* (36), *GFP* (37), *Sema3a* MT (6× myc-tag) (38) and *Twist* (39). *SEMA3A* constructs were synthesized and cloned into the pcDNA3.1/*myc*-His B vector: human SEMA3A wt, human SEMA3A c.196C>T (p.R66W), human SEMA3A c.2002A>G (p.I668V). For the knockdown experiments, the following MO were used: chd7 MO (5′-AACTCATCA TGCCAGGGTCTGCCAT-3′), sema3a MO (5′-GCAATCCAGGTCAGA GAGCCCATGC-3′), standard control MO (5′-CCTCTTACCTCAGTT ACAATTTATA-3′) (Gene Tools, LLC).

Embryos were injected in one blastomere at the two-cell stage for *in situ* hybridization and analysis of craniofacial structures. *β-galactosidase* (*lacZ*) mRNA, coding for the enzyme bacterial β-galactosidase, was co-injected as a lineage tracer. After fixation in MEMFA (3.7% formaldehyde, 0.1 M MOPS, 2 mM EGTA, 1 mM $MgSO_4$), X-gal staining was performed as described (34,40). Whole mount *in situ* hybridization was performed according to previous protocols (40), using a Digoxigenin labeled *Twist* antisense RNA probe to mark neural crest cells. Embryos for RT-PCR were injected in both blastomeres at the two-cell stage, and neural crest explants were dissected at premigratory neural crest cell stages. For the Chd7 loss-of-function rescue experiments, different combinations of chd7 MO or control MO (5 ng) and *SEMA3A* or *GFP* mRNA constructs (250 pg) were injected as indicated in the figure legends. *GFP* overexpression served as a negative control. Embryos were cultivated until stage 38–42 and phenotypically analyzed for craniofacial defects.

### RT-PCR of *Xenopus* neural crest explants

For RT-PCR embryos were co-injected with 10 ng control MO or chd7 MO and 50 pg *GFP* RNA as a lineage tracer. A total of 100 cranial neural crest explants per condition were dissected from both sides of injected embryos at stages 17–18 as described (41) and immediately frozen in liquid nitrogen. RNA isolation was performed using the Illustra RNAspin Mini Kit (GE Healthcare). MuLV Reverse Transcriptase (Thermo Fisher Scientific) was used for cDNA synthesis. RT-PCR for *histone H4* and *sema3a* was conducted with the following primer-pairs: H4_fw CGGGATA ACATTCAGGGTATCACT, H4_rv ATCCATGGCGGTAACTGTCTTC CT, Sema3a_fw TACATTGGCTCGTCAGTGGG, Sema3a_rv AAA ACTAGGGCACGCTGTGA. PCR was performed with 32–35 cycles using the DreamTaq DNA Polymerase (Thermo Fisher Scientific). Quantitative analysis of PCR-bands was carried out via the Image Studio software of Odyssey® Fc Imaging System (LI-COR Bioscience). The ratio between *Sema3a* and *histone H4* expression was calculated to normalize for initial variations in sample concentration.

### Patients

Thirty-one patients were included in the study, from which 17 were recruited from the University Medical Center Groningen (UMCG). Patients with a confirmed *CHD7* mutation were selected from whom DNA was available. The patients were grouped in typical or atypical CHARGE patients according to the clinical criteria of Blake (22) and/or Verloes (23). The collaboration to this study has been exempted from ethical review by the Medical Ethical Review Committee of the UMCG and UMG.

## Supplementary Material

Supplementary Material is available at *HMG* online.

## Acknowledgements

We thank all patients and their parents for participating in this research project and Johanna Mänz for excellent technical assistance.

*Conflict of Interest statement*. None declared.

## Funding

This work was supported by the Deutsche Forschungsgemeinschaft (DFG) grants PA 2030/1-3 to S.P. and BO 1978/5-1 to A.B.

## References


1. Kolodkin, A.L., Matthes, D.J. and Goodman, C.S. (1993) The semaphorin genes encode a family of transmembrane and secreted growth cone guidance molecules. *Cell*, **75**, 1389–1399.
2. (1999) Unified nomenclature for the semaphorins/collapsins. Semaphorin Nomenclature Committee. *Cell*, **97**, 551–552.
3. Schwarz, Q., Vieira, J.M., Howard, B., Eickholt, B.J. and Ruhrberg, C. (2008) Neuropilin 1 and 2 control cranial gangliogenesis and axon guidance through neural crest cells. *Development (Cambridge, England)*, **135**, 1605–1613.
4. Anderson, R.B., Bergner, A.J., Taniguchi, M., Fujisawa, H., Forrai, A., Robb, L. and Young, H.M. (2007) Effects of different regions of the developing gut on the migration of enteric neural crest-derived cells: a role for Sema3A, but not Sema3F. *Dev. Biol.*, **305**, 287–299.
5. Osborne, N.J., Begbie, J., Chilton, J.K., Schmidt, H. and Eickholt, B.J. (2005) Semaphorin/neuropilin signaling influences the positioning of migratory neural crest cells within the hindbrain region of the chick. *Dev. Dyn.*, **232**, 939–949.
6. Eickholt, B.J., Mackenzie, S.L., Graham, A., Walsh, F.S. and Doherty, P. (1999) Evidence for collapsin-1 functioning in the control of neural crest migration in both trunk and hindbrain regions. *Development (Cambridge, England)*, **126**, 2181–2189.
7. Dodé, C. and Hardelin, J.-P. (2009) Kallmann syndrome. *Eur. J. Hum. Genet.: EJHG*, **17**, 139–146.
8. Hanchate, N.K., Giacobini, P., Lhuillier, P., Parkash, J., Espy, C., Fouveaut, C., Leroy, C., Baron, S., Campagne, C., Vanacker, C. *et al.* (2012) SEMA3A, a gene involved in axonal pathfinding, is mutated in patients with Kallmann syndrome. *PLoS Genet.*, **8**, e1002896.
9. Känsäkoski, J., Fagerholm, R., Laitinen, E.-M., Vaaralahti, K., Hackman, P., Pitteloud, N., Raivio, T. and Tommiska, J. (2014) Mutation screening of SEMA3A and SEMA7A in patients with congenital hypogonadotropic hypogonadism. *Pediatr. Res.*, **75**, 641–644.
10. Dodé, C. and Hardelin, J.-P. (2010) Clinical genetics of Kallmann syndrome. *Ann. D'endocrinol.*, **71**, 149–157.
11. van Battum, E.Y., Brignani, S. and Pasterkamp, R.J. (2015) Axon guidance proteins in neurological disorders. *Lancet Neurol.*, **14**, 532–546.
12. Chalouhi, C., Faulcon, P., Le Bihan, C., Hertz-Pannier, L., Bonfils, P. and Abadie, V. (2005) Olfactory evaluation in children: application to the CHARGE syndrome. *Pediatrics*, **116**, e81–e88.
13. Pinto, G., Abadie, V., Mesnage, R., Blustajn, J., Cabrol, S., Amiel, J., Hertz-Pannier, L., Bertrand, A.M., Lyonnet, S., Rappaport, R. *et al.* (2005) CHARGE syndrome includes hypogonadotropic hypogonadism and abnormal olfactory bulb development. *J. Clin. Endocrinol. Metab.*, **90**, 5621–5626.
14. Ogata, T., Fujiwara, I., Ogawa, E., Sato, N., Udaka, T. and Kosaki, K. (2006) Kallmann syndrome phenotype in a female patient with CHARGE syndrome and CHD7 mutation. *Endocrine J.*, **53**, 741–743.
15. Bergman, J.E.H., Bosman, E.A., van Ravenswaaij-Arts, C.M.A. and Steel, K.P. (2010) Study of smell and reproductive organs in a mouse model for CHARGE syndrome. *Eur. J. Hum. Genet.*, **18**, 171–177.
16. Jongmans, M.C.J., van Ravenswaaij-Arts, C.M.A., Pitteloud, N., Ogata, T., Sato, N., Claahsen-van der Grinten, H.L., van der Donk, K., Seminara, S., Bergman, J.E.H., Brunner, H.G. *et al.* (2009) CHD7 mutations in patients initially diagnosed with Kallmann syndrome–the clinical overlap with CHARGE syndrome. *Clin. Genet.*, **75**, 65–71.
17. Schulz, Y., Wehner, P., Opitz, L., Salinas-Riester, G., Bongers, E.M.H.F., van Ravenswaaij-Arts, C.M.A., Wincent, J., Schoumans, J., Kohlhase, J., Borchers, A. *et al.* (2014) CHD7, the gene mutated in CHARGE syndrome, regulates genes involved in neural crest cell guidance. *Hum. Genet.*, **133**, 997–1009.
18. Payne, S., Burney, M.J., McCue, K., Popal, N., Davidson, S.M., Anderson, R.H. and Scambler, P.J. (2015) A critical role for the chromatin remodeller CHD7 in anterior mesoderm during cardiovascular development. *Dev. Biol.*, **405**, 82–95.
19. Hofmann, K., Zweier, M., Sticht, H., Zweier, C., Wittmann, W., Hoyer, J., Uebe, S., van Haeringen, A., Thiel, C.T., Ekici, A.B. *et al.* (2013) Biallelic SEMA3A defects cause a novel type of syndromic short stature. *Am. J. Med. Genet. A*, **161A**, 2880–2889.
20. Baumann, M., Steichen-Gersdorf, E., Krabichler, B., Müller, T. and Janecke, A.R. (2017) A recognizable type of syndromic short stature with arthrogryposis caused by bi-allelic SEMA3A loss-of-function variants. *Clin. Genet.*, **92**, 86–90.
21. Bajpai, R., Chen, D.A., Rada-Iglesias, A., Zhang, J., Xiong, Y., Helms, J., Chang, C.-P., Zhao, Y., Swigut, T. and Wysocka, J. (2010) CHD7 cooperates with PBAF to control multipotent neural crest formation. *Nature*, **463**, 958–962.
22. Blake, K.D., Davenport, S.L., Hall, B.D., Hefner, M.A., Pagon, R.A., Williams, M.S., Lin, A.E. and Graham, J.M. (1998) CHARGE association: an update and review for the primary pediatrician. *Clin. Pediatrics*, **37**, 159–173.
23. Verloes, A. (2005) Updated diagnostic criteria for CHARGE syndrome: a proposal. *Am. J. Med. Genet. A*, **133A**, 306–308.
24. Adams, R.H., Lohrum, M., Klostermann, A., Betz, H. and Püschel, A.W. (1997) The chemorepulsive activity of secreted semaphorins is regulated by furin-dependent proteolytic processing. *EMBO J.*, **16**, 6077–6086.
25. Plein, A., Calmont, A., Fantin, A., Denti, L., Anderson, N.A., Scambler, P.J. and Ruhrberg, C. (2015) Neural crest-derived SEMA3C activates endothelial NRP1 for cardiac outflow tract septation. *J. Clin. Invest.*, **125**, 2661–2676.
26. Ishii, M., Arias, A.C., Liu, L., Chen, Y.-B., Bronner, M.E. and Maxson, R.E. (2012) A stable cranial neural crest cell line from mouse. *Stem Cells Dev.*, **21**, 3069–3080. 10.1089/scd.2012.0155.
27. Bronner, M.E. and Simoes-Costa, M. (2016) The neural crest migrating into the twenty-first century. *Curr. Topics Dev. Biol.*, **116**, 115–134.
28. Tannous, A., Pisoni, G.B., Hebert, D.N. and Molinari, M. (2015) N-linked sugar-regulated protein folding and quality control in the ER. *Semin. Cell Dev. Biol.*, **41**, 79–89.
29. Jongmans, M.C.J., Admiraal, R.J., van der Donk, K.P., Vissers, L.E.L.M., Baas, A.F., Kapusta, L., van Hagen, J.M., Donnai, D., Ravel, TJ. d., Veltman, J.A. *et al.* (2006) CHARGE syndrome: the phenotypic spectrum of mutations in the CHD7 gene. *J. Med. Genet.*, **43**, 306–314.
30. Sanlaville, D., Etchevers, H.C., Gonzales, M., Martinovic, J., Clément-Ziza, M., Delezoide, A.-L., Aubry, M.-C., Pelet, A., Chemouny, S., Cruaud, C. *et al.* (2006) Phenotypic spectrum of CHARGE syndrome in fetuses with CHD7 truncating mutations correlates with expression during human development. *J. Med. Genet.*, **43**, 211–217.
31. Legendre, M., Abadie, V., Attié-Bitach, T., Philip, N., Busa, T., Bonneau, D., Colin, E., Dollfus, H., Lacombe, D., Toutain, A.

*et al*. (2017) Phenotype and genotype analysis of a French cohort of 119 patients with CHARGE syndrome. *Am. J. Med. Genet. C, Semin. Med. Genet.* **175**, 417–430.
32. Hofemeister, H., Ciotta, G., Fu, J., Seibert, P.M., Schulz, A., Maresca, M., Sarov, M., Anastassiadis, K. and Stewart, A.F. (2011) Recombineering, transfection, Western, IP and ChIP methods for protein tagging via gene targeting or BAC transgenesis. *Methods (San Diego, Calif.)*, **53**, 437–452. 10.1016/j.ymeth.2010.12.026.
33. Tian, B., Yang, J. and Brasier, A.R. (2012) Two-step cross-linking for analysis of protein-chromatin interactions. *Methods Mol. Biol. (Clifton, N.J.)*, **809**, 105–120.
34. Borchers, A., David, R. and Wedlich, D. (2001) Xenopus cadherin-11 restrains cranial neural crest migration and influences neural crest specification. *Development (Cambridge, England)*, **128**, 3049–3060.
35. Nieuwkoop, P.D. and Faber, J., Hubrecht Laboratory Utrecht. (1956) Normal table of Xenopus laevis (Daudin) : a systematical and chronological survey of the development from the fertilized egg till the end of metamorphosis. North-Holland Pub. Co., Amsterdam.
36. Smith, W.C. and Harland, R.M. (1991) Injected Xwnt-8 RNA acts early in Xenopus embryos to promote formation of a vegetal dorsalizing center. *Cell*, **67**, 753–765.
37. Moriyoshi, K., Richards, L.J., Akazawa, C., O'Leary, D.D. and Nakanishi, S. (1996) Labeling neural cells using adenoviral gene transfer of membrane-targeted GFP. *Neuron.*, **16**, 255–260.
38. Campbell, D.S., Regan, A.G., Lopez, J.S., Tannahill, D., Harris, W.A. and Holt, C.E. (2001) Semaphorin 3A elicits stage-dependent collapse, turning, and branching in Xenopus retinal growth cones. *J. Neurosci.*, **21**, 8538–8547.
39. Hopwood, N.D., Pluck, A. and Gurdon, J.B. (1989) A Xenopus mRNA related to Drosophila twist is expressed in response to induction in the mesoderm and the neural crest. *Cell*, **59**, 893–903.
40. Harland, R.M. (1991) In situ hybridization: an improved whole-mount method for Xenopus embryos. *Methods Cell Biol.*, **36**, 685–695.
41. Borchers, A., Epperlein, H.H. and Wedlich, D. (2000) An assay system to study migratory behavior of cranial neural crest cells in Xenopus. *Dev. Genes Evol.*, **210**, 217–222. 10.1007/s004270050307.